Journal of the European Ceramic Society **15** (1995) 801–809

0955-2219/95/$9.50

0955-2219(95)00044-5

Interfacial Reaction in Carbon Fibre–Sialon Ceramic Composites

P. Dupel & A. Hendry

Department of Metallurgy & Engineering Materials, University of Strathclyde, Glasgow, UK

(Received 7 June 1994; revised version received 10 February 1995; accepted 14 February 1995)

Abstract

Sintering and interfacial reaction have been studied in a composite of sialon matrix with chopped carbon fibre reinforcement. It has been shown that at relatively low temperature (1500°C) there is a little α *to* β *transformation in the reaction sintered matrix, no interfacial reaction (the carbon fibre is unaltered by the firing cycle) and 20% apparent porosity. As the temperature is increased to 1550°C and 1600°C, a corresponding increase in both transformation and density occur but accompanied by significant interfacial reaction. The nature of these changes is quantified and the microstructures determined by electron microscopy. The observations are interpreted in terms of interface chemistry, and transport mechanisms in both the gas and liquid phases are explained. Optimised procedures for fabrication are suggested.*

1 Introduction

The development of silicon nitride engineering ceramics over the last two decades has been devoted to the pursuit of maximum sintered density and therefore to the highest levels of mechanical strength. However, of equal importance is the need for reliability and reproducibility in the fabricated component, and for a means of crack inhibition to improve the relative toughness. Both of these aspects can be addressed through the use of composite action in the ceramic matrix, although this will necessarily lead to some decrease in fracture strength. A number of papers devoted to these aspects of the mechanical behaviour of ceramic matrix composites have been published in recent years and these are best summarised in the proceedings of the conferences at Riso[1] and that specifically devoted to silicon nitride in Stuttgart in 1993.[2]

Before detailed modelling of fracture behaviour can be attempted, however, it is necessary to address the problems of composite fabrication. This is necessary because, in general, the systems of interest are chemically incompatible, i.e. a reaction occurs between the matrix and the reinforcement during high-temperature fabrication or high-temperature use. The specific problem of carbon-fibre-reinforced silicon nitride materials was first discussed by Kyotoku *et al.*[3] where the nature of the interfacial reaction was identified and methods of inhibition or prevention devised. The critical factors are the interaction of the sintering gas atmosphere with the composite in the early stages of sintering when open porosity is present, and the rate of pore closure. However, in that work[3] and in subsequent investigations at Strathclyde, the detailed nature of the carbon–sialon interaction was not elucidated and therefore the micromechanisms at the interface are not known. There are specific requirements for knowledge of (i) the influence of temperature on the interfacial reaction, (ii) the interaction between sintering mechanisms and interfacial reaction, and therefore (iii) the role of the sintering liquid phase on material transport at the interface.

In order to have a simple, rapid densification, it was decided to use hot pressing as the fabrication method and to use a limited range of temperatures, 1500–1600°C, in which it was evident that both sintering and interfacial reaction were relatively rapid. The hot-press environment of a graphite die initially heated in air gives rise to a gas atmosphere with total pressure slightly in excess of one atmosphere with a chemical composition of 35 vol.% CO and 65 vol.% N_2 from the conversion of air to nitrogen and carbon monoxide. An investigation was therefore carried out to determine the answers to the three headings above and to provide guidance on the optimum fabrication routes for strong, reliable composites.

2 Experimental Procedure

The composites were prepared from β'-sialon 201 supplied by Cookson Group and containing un-reacted α-Si_3N_4, 6 wt% Al_2O_3, 8 wt% Y_2O_3 (as a densifying aid) and 10 wt% AlN polytypes. During sintering, this material forms a β'-sialon

of composition $Si_{5.25}Al_{0.75}O_{0.75}N_{7.25}$ (β'; $z = 0.75$). Reinforcing material used was chopped carbon fibre supplied by Osaka Gas Co. and two different proportions of carbon fibre have been added to the matrix : 10 vol.% and 20 vol.% The appropriate quantities of matrix and reinforcement material were wet-mixed for 2 h in propan-2-ol using alumina balls. After evaporating the alcohol, the powder was remixed dry for 1 h. Samples were uniaxially cold-compacted in a steel die to approximately 60% of the theoretical density to produce cylindrical pellets (15 mm diameter × 5 mm; 1·5 g). The pellets were embedded in boron nitride powder and hot-pressed in a graphite die under a stress of 30 MPa at different temperatures (1500, 1550 and 1600°C). Temperature was monitored by a two-colour optical pyrometer. The sintering time used was generally 1 h but lower times have also been used to determine the sequence of the reaction. Samples were subsequently sectioned and polished for micro-examination. Densities were measured by Archemedes' method using distilled water. Crystalline phases present were identified by X-ray powder diffraction using a Hägg–Guinier focusing camera (CuK_α, 50 KV, 20 mA). The microstructure of the samples has been studied by scanning electron microscopy (SEM, Jeol 840) and by transmission electron microscopy (TEM, Philips 400T) equipped with a windowless energy-dispersive X-ray analysis system (EDX).

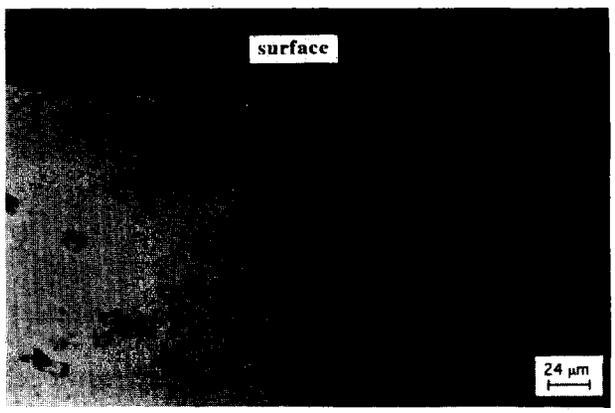

Fig. 1a. Optical micrograph of a 10 vol.% fibre composite sintered at 1550°C for 1 h, showing the external surface of the compact.

Fig. 1b. Optical micrograph of a 10 vol.% fibre composite sintered at 1600°C for 1 h.

3 Results

3.1 Density, weight losses and optical observations of the samples

Table 1 gives the densities and weight losses of samples sintered for 1 h at various temperatures and containing 10 or 20 vol.% carbon fibres.

The weight loss and density increase slightly for a given temperature with the amount of fibre in the sample. At 1500°C, the weight loss is negligible and density is very low, while the maximum density is obtained from 1550°C and the weight loss increases slightly with temperature. It should be noted that the percentage of theoretical density is sensitive to the value assumed for theoretical density. The value for density of carbon fibre given by the manufacturer is an overestimate of the true value, and samples fired at 1600°C are effectively fully dense. All weight losses are very small.

Table 1. Sample density and weight loss for various sintering temperatures and carbon fibre loadings

	Vol.% fibre		*Vol.% fibre*	
	10	*20*	*10*	*20*
Temperature (°C)	*Density (% theoretical)*		*Weight loss (%)*	
1500	81	83	0·2	0·4
1550	92	94	1·3	1·7
1600	94	95	2·0	2·5

Accuracy of density ±1%, weight loss ±0·2%.

Samples sintered at 1600°C exhibit a grey colour in contrast to the black colour at lower temperatures. Optical micro-observations show that at 1600°C and 1550°C a reaction has taken place between the matrix and the carbon fibre and at 1600°C an external surface layer is formed as shown in Figs 1a and 1b, respectively.

3.2 SEM observations

Electron microscopy observations of samples sintered for 1 h at 1500°C confirm a weak reaction between fibres and matrix. Cross-sectional and surface appearance of fibres do not reveal any attack, and the matrix appears to be adherent to the fibres as shown in Figs 2a and 2b. At 1550°C with 10 vol.% fibre, two kinds of fibre are observed. First, fibres with a reaction layer between the carbon core and the matrix, as shown in Fig 3. Usually small pores are also present between the matrix and the reaction layer. Second, some fibres do not seem to have reacted with the matrix and

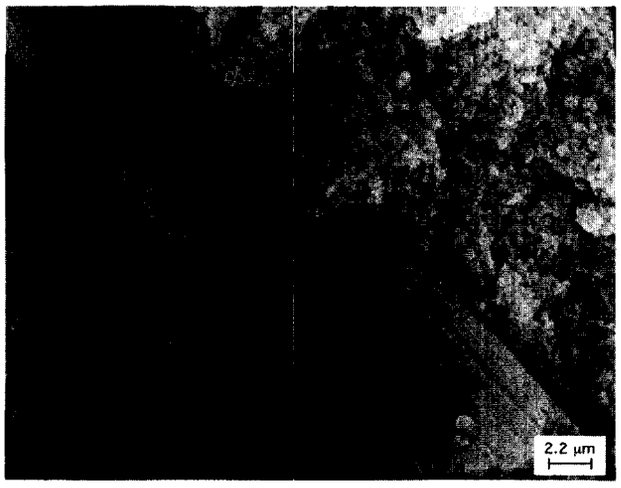

Fig. 2a. SEM micrograph of the external surface of a fibre in a 10 vol.% fibre composite sintered at 1500°C for 1 h.

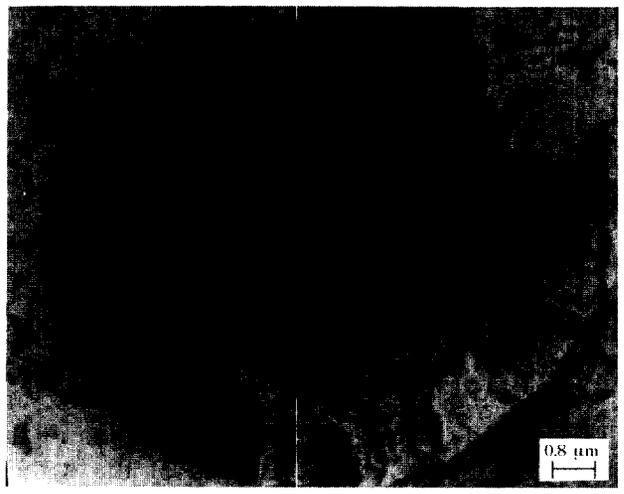

Fig. 2b. SEM micrograph of a cross-section of a fibre in a 10 vol.% fibre composite sintered at 1500°C for 1 h.

show the same appearance as in Figs 2a and 2b. Samples with 20 vol.% fibres and fired at the same temperature exhibit a similar comportment but the reaction between the matrix and the fibre is less extensive. It should also be noted that independent from the fibre loading, fibres near the

Fig. 3. As in Fig. 2 sintered at 1550°C for 1 h.

Fig. 4. As in Fig. 2 and 3 sintered at 1600°C for 1 h.

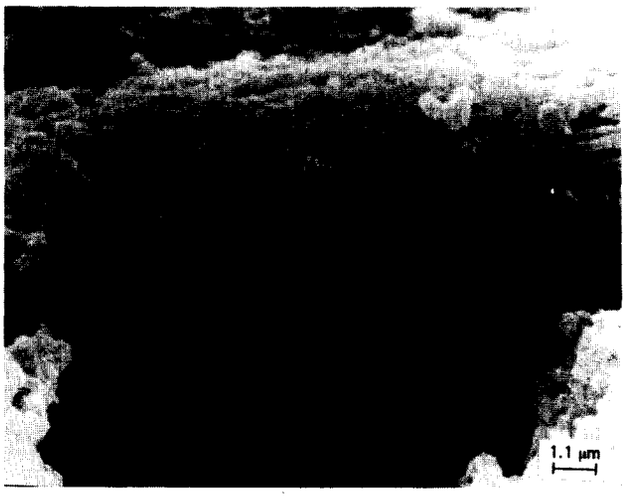

Fig. 5. SEM micrograph of the external surface of a reacted fibre in a 10 vol.% fibre composite sintered at 1600°C for 1 h.

surface of the pellet appear to be more heavily attacked than at the centre (see also Fig. 1b).

At 1600°C for 1 h with 10 vol.% of fibres, the reaction is more extended and complete for most of the fibres, i.e. the initial structure of the carbon fibre is no longer apparent, as shown in Fig 4. In this case, there is extensive porosity around the fibre and the surface of the fibres exhibit holes due to gas emission, as shown in Fig. 5. There is no difference between the surface and the centre of the pellet after 1 h, but a sample fired at 1600°C for only 5 min reveals a less extensive reaction and a clear difference between the surface and the centre of the pellet. As at 1550°C, samples with 20 vol.% fibres sintered at 1600°C create a less-extended reaction than the 10 vol.% fibres.

3.3 T.E.M. and X-ray analysis

3.3.1 Matrix

Figure 6 shows the X-ray diffraction patterns obtained from samples containing 10 vol.% fibres

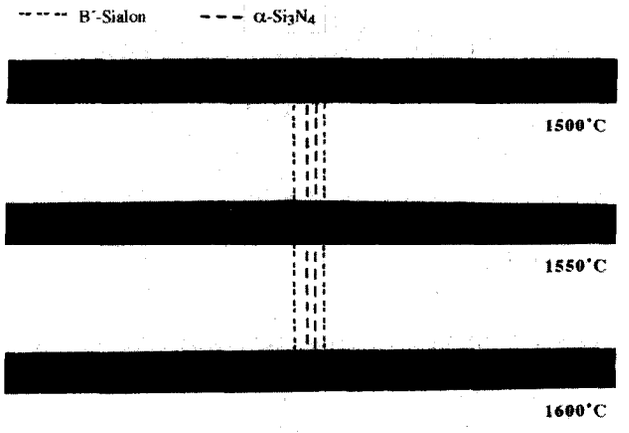

Fig. 6. X-ray Guinier camera photographs of 10 vol.% fibre composites fired at three different temperatures for 1 h.

and sintered at various temperatures for 1 h. As expected, there is a large variation in the sample composition with temperature since at 1500°C α-Si_3N_4 is the main phase, whereas at 1600°C β'-sialon is in the majority. The z-value of the β' phase calculated from the β' lines of the diffraction patterns presented in Fig. 6 follows the variation with temperature as shown in Table 2. The lower the temperature, the higher the z-value. A variation is also observed with the amount of carbon fibres.

TEM observations of the matrix corroborate the X-ray analysis. At 1500°C, large α-Si_3N_4 grains are surrounded by smaller grains and the

Table 2. β'-sialon z-value and main phases versus sintering temperature and fibre content

Temperature (°C)	*v/o fibre*		*Main phases*
	10	*20*	
	z-Value		
1500	0·92	1·33	α-Si_3N_4 (tr. β'-sialon)
1550	0·77	1·06	α-Si_3N_4 + β'-sialon
1600	0·46	0·72	β'-sialon

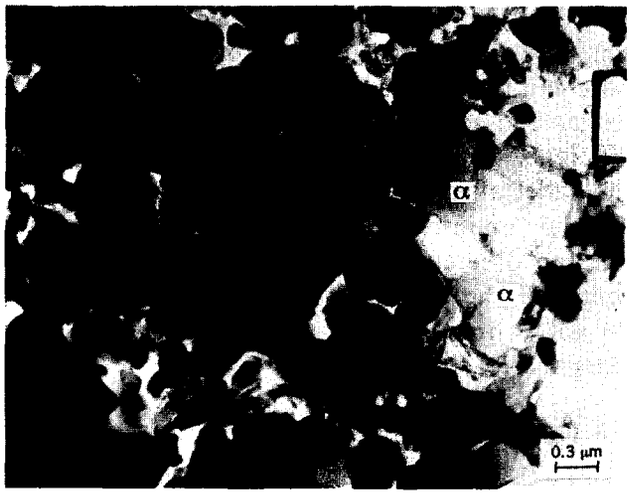

Fig. 7. TEM bright field micrograph of the matrix of a 10 vol.% fibre composite sintered at 1500°C for 1 h, showing residual α-$Si_3x/4$ grains.

Fig. 8. TEM bright field micrograph of the matrix of a 20 vol.% fibre composite sintered at 1600°C for 1 h.

sample exhibits a low density as shown in Fig. 7. Some elongated β'-sialon crystals are also present. At higher temperature, the matrix is more dense and no large α-Si_3N_4 grains are observed, as shown in Fig. 8.

3.3.2 Carbon fibre–matrix interface

At 1500°C, whatever the content of fibre, most of the carbon fibres have not reacted with the matrix. A typical interface between the two components is shown in Fig. 9. The fibre and the matrix are clearly unreacted and the low densification of the matrix is obvious. EDX analysis of the carbon fibre gives only a carbon peak and a small silicon peak (see Fig. 10). However, in some places in the sample, two other features of the fibres can be observed. First, the carbon fibre reveals a weak reaction with the components of the matrix, particularly the liquid phase, giving rise to very tiny grains at the interface or within the fibre, as shown in Fig. 11a. EDX analysis shows that these

Fig. 9. TEM bright field micrograph of a fibre–matrix interface in a 10 vol.% composite sintered at 1500°C for 1 h.

small grains and the fibre itself contain a larger amount of silicon than the unreacted fibre, as shown in Fig. 11b. In rare places, some large pieces of silicon carbide with intergrowths are observed, as shown in Fig. 12.

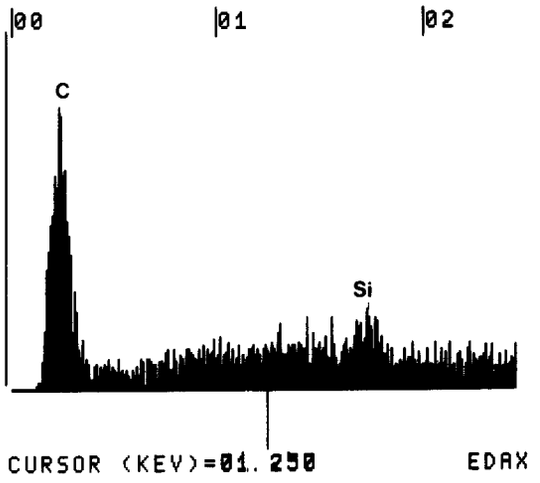

Fig. 10. Energy-dispersive analysis trace of the carbon fibre shown in Fig. 9.

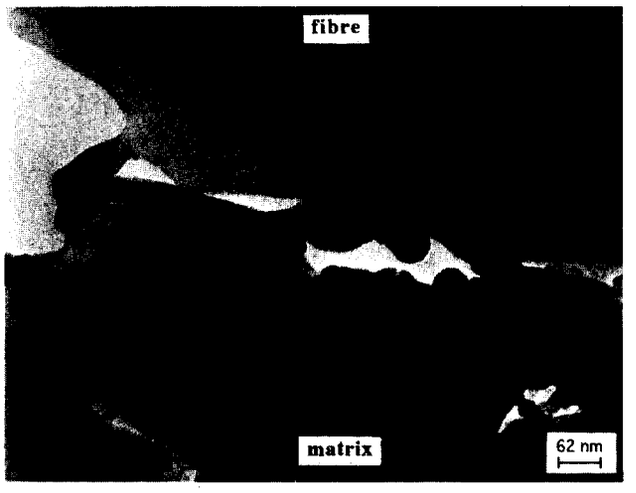

Fig. 11a. TEM bright field micrograph of the fibre–matrix interface in a 10 vol.% fibre composite fired at 1550°C for 1 h.

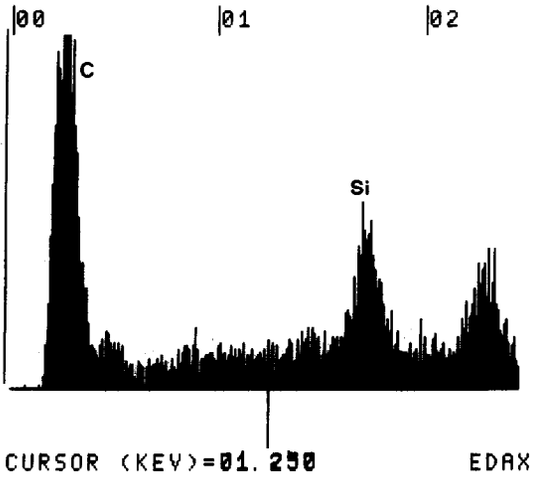

Fig. 11b. Energy-dispersive analysis trace of the carbon fibre shown in Fig. 11a.

A higher temperature, 1600°C, yielded a noticeably different microstructure in that extensive reaction had taken place between matrix and fibre. Two main structures are observed in the samples. First, some net interfaces between the fibre and

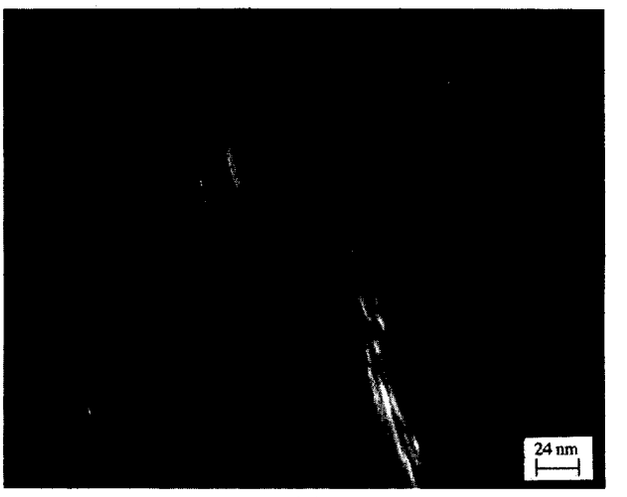

(a)

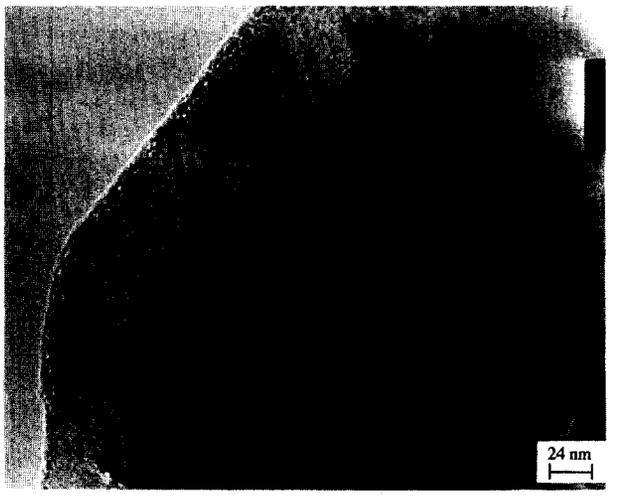

(b)

Fig. 12. Bright field (a) and dark field (b) TEM micrographs of fibre containing faulted silicon carbide.

Fig. 13. TEM bright field micrograph of the fibre–matrix interface in a 20 vol.% fibre composite sintered at 1600°C for 1 h.

the matrix are seen, as shown in Fig 13. As at lower temperatures, the carbon fibre contains silicon. The matrix contains a large amount of liquid phase containing Y, Si, Al and O (see Fig. 14) and small grains are embedded in this solidified liquid as shown in Fig 15a. Generally, few silicon carbide grains are observed in the samples fired at 1600°C for 1 h, and in this case they are located in the matrix or surrounded by the solidified liquid phase (see arrow in Fig. 15a). However, when the sintering time is shorter, 5 min, some large areas containing a lot of SiC grains are found as shown in Fig. 15b (silicon carbide grains are clearly evident from the high incidence of faulting). The second main structure observed is presented in Fig. 16a. This reacted carbon fibre shows a peculiar appearance with very small grains within the structure. The EDX analysis of the carbon fibre shows the presence of silicon and more surprisingly of molybdenum. These products are found again in some other places in the matrix, as shown in Fig. 16b (see arrow). The diffraction patterns of both such areas show that the small grains are SiC. These types of reacted carbon fibre are often observed as a thin film in the matrix, as shown in Fig 17. Whatever the temperature and the carbon content in the sample, some bubbles in the liquid phase are often observed near the fibre–matrix interfaces as, shown in Fig. 18.

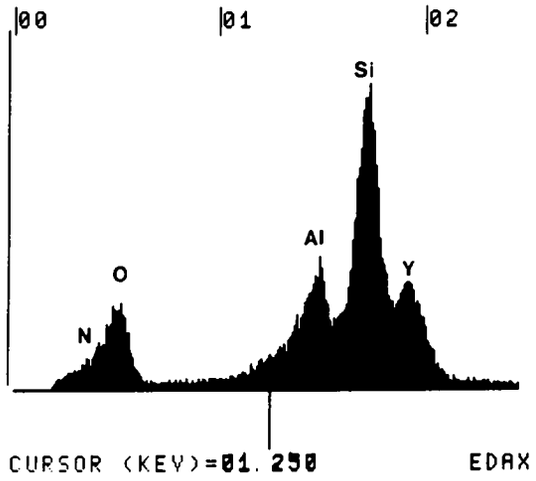

Fig. 14. Energy-dispersive analysis of a glassy phase area in Fig. 13.

Fig. 15a. Bright field TEM micrograph of precipitation of SiC (arrow) from the liquid phase in a 20 vol.% fibre composite sintered at 1600°C for 1 h.

Fig. 15b. TEM bright field micrograph of silicon carbide grains in a 10 vol.% fibre composite sintered at 1600°C for 5 min.

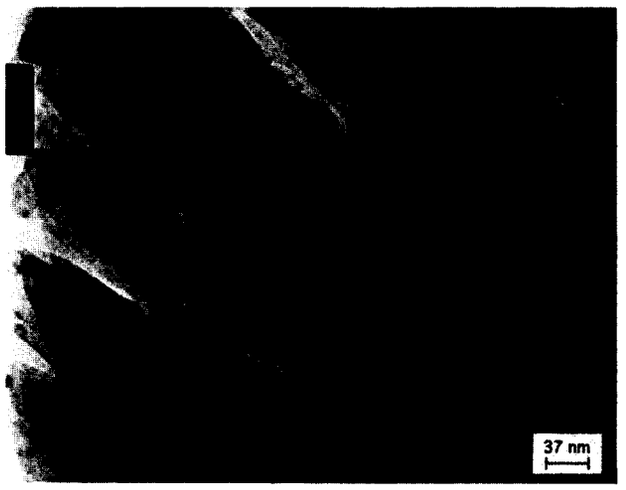

Fig. 16a. TEM bright field micrograph c/a reacted fibre in a 10 vol.% fibre composite sintered at 1600°C for 1 h.

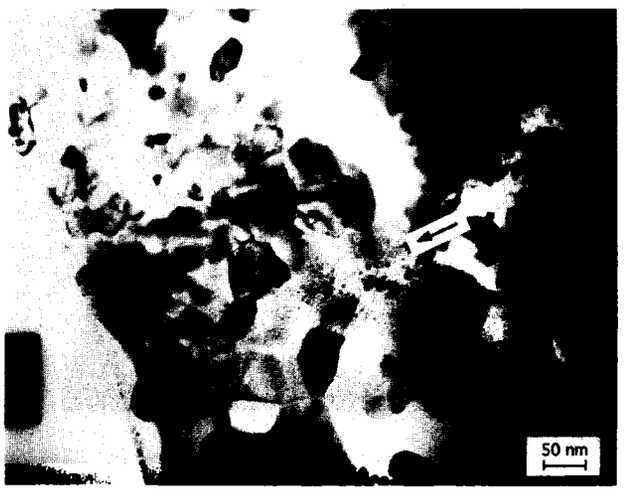

Fig. 16b. TEM bright field micrograph of a 20 vol.% fibre composite sintered at 1600°C for 1 h.

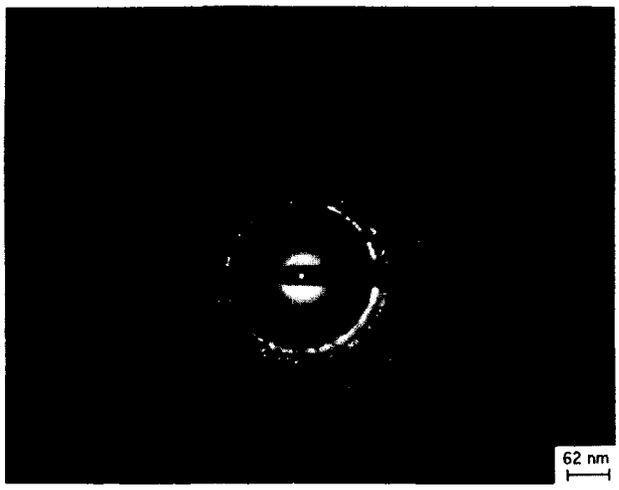

Fig. 16c. Electron diffraction pattern of silicon carbide grains in a fibre from a composite sintered at 1600°C for 1 h.

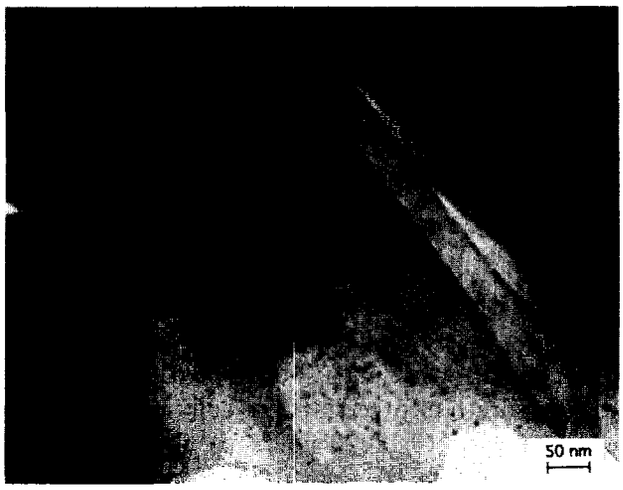

Fig. 17. TEM bright field micrograph of a 10 vol.% fibre composite sintered at 1600°C for 5 min.

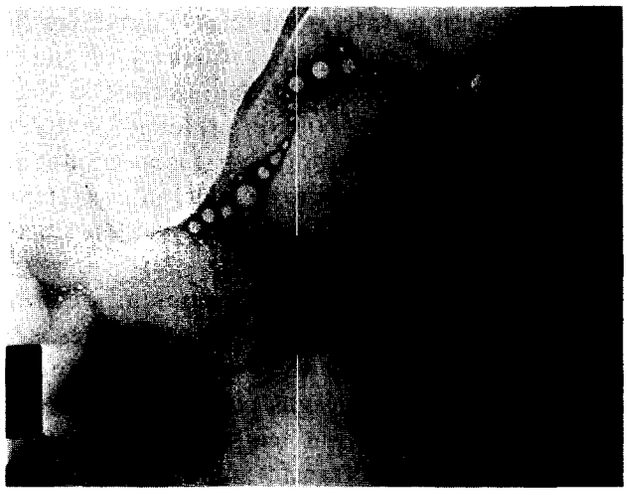

Fig. 18. TEM bright field micrograph of gas pores in the liquid phase of a 20 vol.% fibre composite sintered at 1600°C.

4 Discussion

It is clear that temperature affects both sintering of the matrix and reaction between the components of the composite, and that sintering only occurs if the temperature is equal to or higher than 1550°C. The interesting result regarding sintering is the variation of the β'-sialon z-value with temperature and with the fibre content. When temperature increases, z decreases. According to Kim and coworkers,[4] this is due to the transformation of α to β' in the matrix. At the beginning of sintering, the liquid phase and the precipitated β'-sialon grains are very Al rich. Because the aluminium in the liquid phase is consumed with the formation of β'-sialon by reaction of α-Si_3N_4 grains, the liquid contains less and less aluminium as the transformation progresses and the Al content in the β'-sialon grains decrease with time. Moreover, the Al-rich β'-sialon grains precipitated at the beginning of sintering redissolve as the Al concentration in the liquid phase decreases. In short, as α dissolves the z-value decreases, and therefore the average z-value of the β'-sialon in the composites decreases with time and temperature. However, some silicon is also consumed by formation of SiC within the fibres during sintering and there the z-value of the matrix β' is expected to decrease with increasing fibre content. That is, the dependence of z with the amount of carbon fibre in the sample is related to the reaction between the matrix and the fibres. Two factors have to be considered. First, the more carbon fibre in the composite, the less liquid phase is present. Second, silicon is incorporated in the attacked fibres (see Fig. 11). So, at a given temperature, the 20 vol.% composite contains more fibres, less liquid phase and Si reacts partly with the fibres. As a consequence, the ratio Si/Al in the liquid phase is lower, the transformation α to β' slower and the z-value is higher for a given sintering time.

From the results, it is clear that the extent of reaction increases with temperature of sintering and is related to the sintering behaviour in that it is promoted by the presence of liquid phase. At low temperature, the extent of sintering is limited and little α to β' transformation occurs, but the β' which is formed is of higher z-value than expected, as discussed above. There is no reaction at 1500°C and the fibre is unaffected by the sintering process. As the temperature and extent of densification increase, so the z-value of β' decreases and the attack on the carbon fibre becomes more pronounced. Two effects on the fibre are clear from the results. First, there is surface degradation due to the attack at the liquid/fibre interface which results in increased porosity in the fibre (compare Figs 5 and 2a). The second effect is reaction within the fibre, which converts the carbon from an amorphous phase to a micropolycrystalline state and includes formation of silicon carbide (Figs 12a and 16a). At the same temperature, as

shown in Fig. 15, there is reaction within the ceramic phase to form grains of silicon carbide as discreet crystals close to the interface. In the relatively short time duration of the present experiments (1 h) it is unlikely that such effects can be explained by liquid-phase diffusion and therefore gaseous transport must be involved both within the ceramic matrix pore network and in the increasingly porous fibres. The gases involved in the sintering environment are N_2 and CO and these must be involved in the process at the earliest stages when open porosity is present. This behaviour has been discussed by Kyotoku *et al.*[3] and it has been shown that in the presence of a significant CO pressure, the interfacial reaction is inhibited and weight losses are therefore expected to be small, as is found in the gas atmosphere of the hot press used in the present experiments. Similarly, open porosity is necessary for a gas evolution reaction (see weight losses in Table 1) at the fibre surface. In addition, however, the strongly reducing environment at the fibre/matrix interface (solid carbon, gaseous CO and N_2) will lead to carbothermal reduction of the predominantly oxide sintering liquid with formation of silicon monoxide (SiO) and carbon monoxide (CO)

$$SiO_2 + C_{(s)} \Leftrightarrow SiO_{(g)} + CO_{(g)} \quad (1)$$

where SiO_2 represents silica at reduced activity in the liquid phase. By this means carbon is consumed at the fibre surface and silicon is transported into the fibres by gaseous diffusion of SiO within the fibre pore network. This reacts with the fibres producing SiC in the fibre structure:

$$SiO_{(g)} + 2C_{(s)} \Leftrightarrow SiC_{(s)} + 2CO_{(g)} \quad (2)$$

while silicon carbide may be formed in the liquid phase either by direct reduction:

$$SiO_2 + 3C_{(s)} \Leftrightarrow SiC_{(s)} + 2CO_{(g)} \quad (3)$$

or by gaseous reaction with the carbon monoxide

$$SiO_2 + 4CO_{(s)} \Leftrightarrow SiC_{(s)} + 3CO_{2(g)} \quad (4)$$

The latter reaction is unlikely, however, both on thermochemical grounds (at 1600°C) and from electron microscopy, which shows that SiC crystals in the ceramic matrix are only found in the immediate vicinity of the interface, indicating reaction with solid carbon. As sintering proceeds and closed porosity develops, all of the above gas-generating reactions will be inhibited as the internal pore pressures increase and further reaction will not occur. Indeed, it should be noted that weight losses are small (Table 1) and that the above reactions are limited in extent even at the highest temperature studied; this is reflected in the high density achieved at 1550 and 1600°C even when reaction occurs.

In a second, later stage of the sintering process, silicon carbide crystals in the matrix redissolve as the system tends toward chemical equilibrium. At 1600°C and below, silicon carbide is thermodynamically unstable with respect to carbon, β'-sialon and the liquid phase.[5–7] The latter is assumed to be in equilibrium with the crystalline solid β' precipitated from it as part of the reaction sintering process.

The optimum manufacturing conditions for such composites require a rapid sintering process and sufficient time at a temperature high enough to equilibrate β'-sialon/liquid. Therefore, to produce a composite with minimum interfacial reaction, the sintering conditions should be arranged so as to provide rapid pore closure, i.e. a fast heating rate and adequate liquid phase. Prolonged sintering should not affect the reaction but is necessary for maximum density and phase transformation. The results also suggest that the fibre composites can be sintered to maximum density at 1600°C, which is 50–100°C less than that recommended for the monolithic ceramic.

5 Conclusion

The present work has shown that good-quality carbon-fibre-reinforced sialon composites can be prepared with 10 or 20 vol.% of fibre. Interfacial reaction between the constituents only takes place above 1500°C, in the temperature range required for liquid-phase sintering of the sialon matrix. The interfacial reaction therefore accompanies the α to β' transformation. Interfacial reaction involves the liquid phase and results in formation of silicon carbide in the matrix side of the interface at short times, but these redistribute on prolonged sintering times. Gas phase transport by silicon monoxide from the matrix to the fibres results in conversion of part of the amorphous fibre to crystalline silicon carbide.

The data suggests that the optimum sintering procedure for these chopped fibre composites is to use a rapid heating rate to provide fast pore closure, thereby preventing gas phase transport, and a maximum densification temperature of 1600°C for 1 h to give α to β' transformation and complete sintering of the matrix.

Acknowledgement

The authors are grateful for the provision of support by the University of Strathclyde Research Fund.

References

1. Bentzen, J. J., Bilde-Sovensen, J. B., Christiansen, N., Horsewell, A. & Ralph, B. (eds), *Structural Ceramics: Processing, Microstructure and Properties*. Riso National Laboratory, Roskilde, 1990.
2. Hoffman, M. J., Becker, P. F. & Petzow, G. (eds), *Silicon Nitride 93*. Trans Tech Publications, Aedesmannsdorf, 1993.
3. Kyotoku, H., Morrison, F. C. R. & Hendry, A., Prediction and control of interface reaction. In *Ceramic–Ceramic Composites*. Silicate Industriel, 53, 1988, p. 143.
4. Kim, N. K., Kim, D. Y., Kranzmann, A., Bischoff, E. & Kang, S. J., Variation of aluminium concentration in β'-sialon grains formed during liquid-phase sintering of Si_3N_4–Al_2O_3–Nd_2O_3. *J. Mater. Sci.*, **28** (1993) 4355–8.
5. Hendry, A., Thermodynamics of silicon nitride and oxynitride. *Proc. NATO-ASI Nitrogen Ceramics*, ed. F. L. Riley. Noordhot, Leyden, 1976, p. 183.
6. Hillert, M. & Jonsson, S., Thermodynamic calculation of the Si–N–O system. *Z. Metallk.*, **83** (1992) 648.
7. Hillert,M. & Jonsson, S., Thermodynamic calculation of the Si–N–O system. *Z. Metallk.*, **83** (1992) 720.